displacement process is quite successful when a single such group is present (entries 11-13). The ability to generate in a single step highly functionalized carbocycles amenable to further functional-group manipulation, such as that shown in eq 1, is one of the most important features of this process.

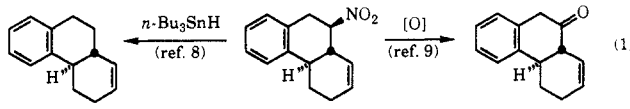

(1)

A wide variety of 1,3-dienes undergo facile, regioselective carboannulation. While we have generally employed 5 equiv of the readily available diene, only slightly reduced yields of carbocycle are obtained when 2 or even 1 equiv of diene is used (Table I, entry 5: 5 equiv, 85%; 2 equiv, 77%; 1 equiv, 76%), but the reaction time is increased substantially (1 day, 6 days, and 7 days, respectively). Simple linear *trans*-dienes afford exclusively the trans olefinic product, but *cis*-1,3-pentadiene affords approximately an 8:1 ratio of *E*:*Z* olefinic products (entry 2).

This carboannulation process most likely proceeds by (1) reduction of $Pd(OAc)_2$ to the actual catalyst Pd(0), (2) oxidative addition of the aryl halide to Pd(0), (3) arylpalladation of the 1,3-diene to form a π-allylpalladium intermediate, and (4) formation of the neighboring carbanion and subsequent front- or backside displacement of palladium, which regenerates the Pd(0) catalyst. The predominant formation of the trans product from *cis*-1,3-pentadiene (entry 2) is best explained by isomerization of an initially formed anti π-allylpalladium intermediate to the more thermodynamically stable syn intermediate.[10] The presence of some cis product, however, suggests that palladium displacement either can occur through a σ-allylpalladium intermediate or is sufficiently rapid to occur via the initially formed anti π-allylpalladium intermediate prior to isomerization. Since all five-membered-ring products contain exclusively cis ring fusion as determined by ^{1}H NMR spectroscopy,[11] they are most likely arising by halide displacement from the initially formed π-allylpalladium intermediate by the tethered nucleophile and subsequent reductive elimination with retention, an unusual path for palladium displacement by stabilized carbanions.[4] All six-membered-ring products contain exclusively a trans ring fusion as determined by ^{1}H NMR spectroscopy,[12] most likely formed by backside palladium displacement.

In conclusion, the simple palladium-catalyzed arylannulation of 1,3-dienes by functionally substituted aryl halides utilizes readily available starting materials and proceeds under mild conditions in high yield, completely stereo- and regioselectively, to form a wide variety of functionally substituted carbocycles.

Acknowledgment. We gratefully acknowledge the National Institutes of Health for their generous financial support and Johnson Matthey, Inc., and Kawaken Fine Chemicals Co., Ltd., for the palladium acetate.

(7) For exceptions, see: (a) Trost, B. M.; Keinan, E. *Tetrahedron Lett.* **1980**, *21*, 2591. (b) Fiaud, J.-C.; Malleron, J.-L. *J. Chem. Soc., Chem. Commun.* **1981**, 159. (c) Negishi, E.; Matsushita, H.; Chatterjee, S.; John, R. A. *J. Org. Chem.* **1982**, *47*, 3188. (d) Negishi, E.; Luo, F.-T.; Pecora, A. J.; Silveira, A., Jr. *J. Org. Chem.* **1983**, *48*, 2427. (e) Negishi, E.; John, R. A. *J. Org. Chem.* **1983**, *48*, 4098.

(8) Larock, R. C. *Comprehensive Organic Transformations: A Guide to Functional Group Preparations*; VCH Publishers: New York, 1989; p 26.

(9) Larock, R. C. *Comprehensive Organic Transformations: A Guide to Functional Group Preparations*; VCH Publishers: New York, 1989; p 603.

(10) Maitlis, P. M.; Espinet, P.; Russell, M. J. H. *Compr. Organomet. Chem.* **1982**, *6*, 385.

(11) The stereochemical assignment is based on the mechanistic argument that backside displacement of palladium by the tethered carbanion would be expected to be stereochemically quite difficult and the fact that the product reported in entry 10 of Table I exhibits J = 6.9 Hz coupling between the two hydrogens on the ring-fused carbons, coupling that is more consistent with cis ring fusion.

(12) Six-membered-ring products, such as the product reported in entry 13 in Table I, which exhibits J = 11.7 Hz coupling between the two hydrogens on the ring-fused carbons, exhibit coupling constants only consistent with an axial-axial arrangement of the two hydrogens.

Supplementary Material Available: General procedure for carboannulation reactions and experimental data (NMR, IR, elemental analysis) for **1-13** (6 pages). Ordering information is given on any current masthead page.

Stereochemical Studies of Coenzyme F430 Based on 2D NOESY Back-Calculations

Karl D. Olson,[†,‡] Hoshik Won,[†] Ralph S. Wolfe,*[,‡] Dennis R. Hare,*[,§] and Michael F. Summers*[,†]

Department of Chemistry and Biochemistry
University of Maryland Baltimore County
Baltimore, Maryland 21228
Department of Microbiology
University of Illinois at Urbana-Champaign
Urbana, Illinois 61801
Hare Research, Inc., 14810 216th Avenue N.E.
Woodinville, Washington 98072

Received January 11, 1990

Coenzyme F430 is a nickel-containing tetrapyrrole from methanogenic bacteria that is utilized in the biocatalytic conversion of CO_2 to methane.[1-6] Although atomic-level structural data for F430 are lacking, elegant one-dimensional (1D) NMR experiments have led to the primary structure determination of the pentamethyl ester derivative (F430M), and 1D nuclear Overhauser effect (NOE) data in combination with chemical data provided a partial stereochemical assignment for the F430M corphin macrocycle.[7-10] The stereochemistry of the C17 carbon (Figure 1) could not be assigned due to severe signal overlap, and the relative stereochemical assignments for C18 and C19 were assigned on the basis of weaker NMR and chemical data and might be considered tentative.[8,11] The C17-C18-C19 stereochemical assignments were determined recently by 2D NMR to be either *R*,*R*,*S* (consistent with the *original* stereochemical assignments) or *S*,*S*,*R* (*reverse* assignment).[12] We describe here the results of a new approach for stereochemical analysis that employs 2D NOESY back-calculations for F430 model structures generated by distance geometry (DG) computations.

DG calculations were performed with DSPACE.[13-16] Covalency constraints dictated by the primary structures of the *original* and

* Authors to whom correspondence should be addressed.
† University of Maryland Baltimore County.
‡ University of Illinois.
§ Hare Research, Inc.

(1) Gunsalus, R. P.; Wolfe, R. S. *FEMS Microbiol. Lett.* **1978**, *3*, 191.
(2) Diekert, G.; Konheiser, U.; Piechulla, K.; Thauer, R. K. *J. Bacteriol.* **1981**, *148*, 459.
(3) Walsh, C. T.; Orme-Johnson, W. H. *Biochemistry* **1987**, *26*, 4901.
(4) Rouviere, P. E.; Wolfe, R. S. *J. Biol. Chem.* **1988**, *263*, 7913.
(5) Bobik, T. A.; Olson, K. D.; Noll, K. M.; Wolfe, R. S. *Biochem. Biophys. Res. Commun.* **1987**, *149*, 455.
(6) Ellermann, J.; Hedderich, R.; Boecher, R.; Thauer, R. K. *Eur. J. Biochem.* **1988**, *172*, 669.
(7) Faessler, A.; Pfaltz, A.; Mueller, P. M.; Farooq, S.; Kratky, C.; Kraeutler, B.; Eschenmoser, A. *Helv. Chim. Acta* **1982**, *65*, 812.
(8) Pfaltz, A.; Jaun, B.; Faessler, A.; Eschenmoser, A.; Jaenchen, R.; Gilles, H. H.; Diekert, G.; Thauer, R. K. *Helv. Chim. Acta* **1982**, *65*, 828.
(9) Livingston, D. A.; Pfaltz, A.; Schreiber, J.; Eschenmoser, A.; Ankel-Fuchs, D.; Moll, J.; Jaenchen, R.; Thauer, R. K. *Helv. Chim. Acta* **1984**, *67*, 334.
(10) Pfaltz, A.; Livingston, D. A.; Jaun, B.; Diekert, G.; Thauer, R. K.; Eschenmoser, A. *Helv. Chim. Acta* **1985**, *68*, 1338.
(11) Eschenmoser, A.; Juan, B.; Pfaltz, A.; Kratky, C., personal communication.
(12) Won, H.; Olson, K. D.; Wolfe, R. S.; Summers, M. F. *J. Am. Chem. Soc.* **1990**, *112*, 2178.
(13) Hare Research, Inc., 14810 216th Ave. N.E., Woodinville, WA 98072.

0002-7863/90/1512-5884$02.50/0

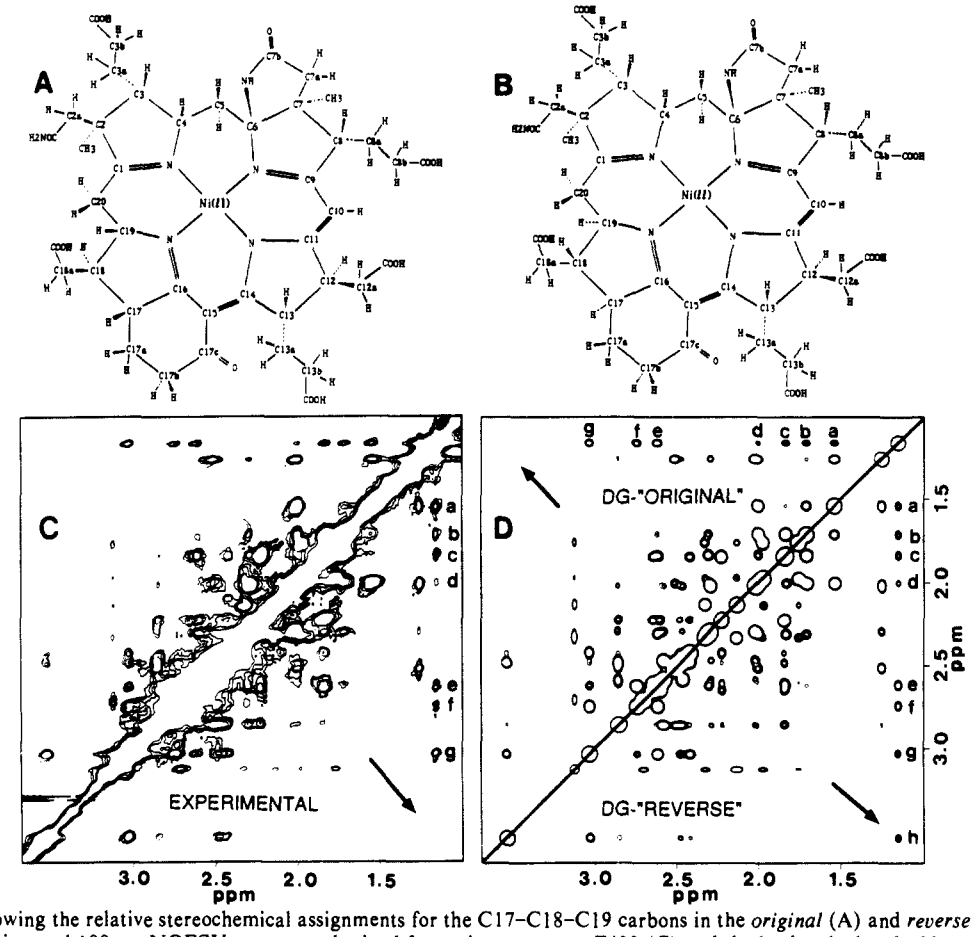

Figure 1. Chart showing the relative stereochemical assignments for the C17–C18–C19 carbons in the *original* (A) and *reverse* (B) structures. Also shown are the experimental 100-ms NOESY spectrum obtained for native coenzyme F430 (C) and the back-calculated 100-ms NOESY spectra for DG structures generated with the *original* (top left) and *reverse* (bottom right) C17–C18–C19 stereochemistries (D). The cross peaks are labeled and assigned as follows: a, H5s; b, H3ar; c, H3as; d, H5r; e, H2as and H3 (overlap); f, H2ar; g, H20r,s; and h, H19.

reverse models were used to generate matrices of allowed upper and lower interatomic distances. Constraints were included to enforce triangle inequality for all triplets of atoms, planarity for conjugated atoms, and Ni–N bond distances of 2.1 Å.[17-21] We found the NOE behavior of the C2 methyl group (Me2, Figure 1) to be diagnostic of the C17–C18–C19 stereochemistry, and interproton distance bounds estimated from cross peaks associated with the Me2 group were included as constraints. Trial distances generated by selecting random distances between the upper and lower bounds for each element were embedded in 3-space with the *metric* matrix method.[22,23] Initial coordinates of the resulting structures, which contained violations of the upper and lower boundary constraints, were refined to minimize deviation with the bounds matrix. Complete refinement was achieved with two additional algorithms, one that adds a random vector of user-specified magnitude (0.2–0.3 Å) to the coordinates of each atom in order to randomize the structure, followed by a simulated annealing refinement algorithm (for more details, see refs 14–16). The complete time course for nuclear relaxation was then determined for each refined structure via numerical integration of the Bloch equations. As described previously,[14] this approach accurately accounts for spin diffusion.

For the *original* model, low-penalty (<0.007 Å^2, =squared sum of all bounds violations) structures were obtained which, when subjected to NOESY back-calculations, provided theoretical spectra with Me2 cross peaks that accurately matched the experimental cross peaks, Figure 1. By adjustment and narrowing of the experimental distance constraints associated with Me2, the buildup of NOE cross peaks and the decay of the diagonal peak with increasing mixing time matched (supplementary material). Final distance constraints from Me2 were as follows: H19, 4.8 Å–infinite; H20s, 3.15–3.25 Å; H2as, 2.95–3.05 Å; H2ar, 2.95–3.05 Å; H3ar, 3.00–3.20 Å; H3as, 3.00–3.20 Å; H5s, 3.00–3.20 Å (r and s indicate *pro-R* and *pro-S* protons, respectively). The fact that low penalties were obtained (maximum penalty = 0.007 Å^2) indicates that the structures do not contain significant van der Waals overlap or unusual (nonideal) bond lengths or bond angles.

Low penalty (ca. 0.02 Å^2) DG structures could be obtained for *reverse* structures by eliminating the Me2–H19 experimental constraint of 4.8 Å–infinity. Although these structures contained only moderate van der Waals and triangularity violations, the back-calculated spectra exhibited a moderate-to-strong Me2-to-H19 cross peak (Figure 1) which was *not* observed experimentally. When constraints were added to push apart the H19–Me2 pair (4.8 Å–infinity), the DG structures exhibited higher penalties (>0.06 Å^2) due to the presence of van der Waals and triangle violations. In particular, as the Me2–H19 distance was increased, the Me2 group came in close contact with the H2ar,s and H3ar,s protons and gave rise to bad geminal and triangle violations for the Me2–C2 bond. The heterocyclic nitrogen atoms and conjugated groups in the resulting structures were distorted significantly

(14) Summers, M. F.; South, T. L.; Kim, B.; Hare, D. R. *Biochemistry* **1990**, *29*, 329.
(15) Nerdal, W.; Hare, D. R.; Reid, B. R. *Biochemistry* **1989**, *28*, 10008.
(16) Banks, K. M.; Hare, D. R.; Reid, B. R. *Biochemistry* **1989**, *28*, 6996.
(17) Diakun, G. P.; Piggott, B.; Tinton, H. J.; Ankel-Fuchs, D.; Thauer, R. K. *Biochem. J.* **1985**, *232*, 281.
(18) Shiemke, A. K.; Shelnutt, J. A.; Scott, R. A. *J. Biol. Chem.* **1989**, *264*, 11236.
(19) Shiemke, A. K.; Hamilton, C. L.; Scott, R. A. *J. Biol. Chem.* **1988**, *263*, 5611.
(20) Eidsness, M. K.; Sullivan, R. J.; Schwartz, J. R.; Hartzell, P. L.; Wolfe, R. S.; Flank, A.; Cramer, S. P.; Scott, R. A. *J. Am. Chem. Soc.* **1986**, *108*, 3120.
(21) Shiemke, A. K.; Scott, R. A. *J. Am. Chem. Soc.* **1988**, *110*, 1645.
(22) Crippen, G. M. *J. Comput. Phys.* **1977**, *24*, 96.
(23) Havel, T. F.; Crippen, G. M.; Kuntz, I. D. *Biopolymers* **1979**, *18*, 73.

from planarity. With these severe structural changes, the Me2 and H19 protons remained sufficiently close to give a weak cross peak in the back-calculated 2D NOESY spectrum (supplementary material).

We have been unable to generate a *reverse* F430 model that is simultaneously consistent with the experimental interproton distance constraints and has low primary covalency violations. Since both structures can be manipulated to be consistent with experimental data, we cannot unambiguously assign the stereochemistry of C19. However, our data indicate that the reverse structure, if it exists, should contain internal strain.

Acknowledgment is made to the donors of the Petroleum Research Fund (Grant ACS-PRF 21219-G3 to M.F.S.), administered by the American Chemical Society, for the partial support of this research. Financial support from the National Science Foundation (1-5-29812 NSF DMB 86-13679 to R.S.W.) and technical support from Victor Gabriel (UIUC), Scott Smith (UIUC), and Jack Suess (UMBC) are gratefully acknowledged.

Supplementary Material Available: Back-calculated 100-ms NOESY spectrum and cross-peak buildup curves associated with Me2 for a representative reverse model generated by inclusion of the Me2–H19 (4.8 Å–infinity) constraint as well as the buildup curves of the cross peaks and decay of the autopeaks associated with the Me2 protons for the experimental, DG "original", and DG "reverse" structures described in Figure 1 (3 pages). Ordering information is given on any current masthead page.

On the Use of Model Compounds To Assess 2-Deoxy-D-*erythro*-pentofuranose Conformation at Apyrimidinic Sites in DNA

A. S. Serianni,* P. C. Kline, and J. R. Snyder

Department of Chemistry and Biochemistry
University of Notre Dame, Notre Dame, Indiana 46556

Received March 14, 1990

The biological mechanisms of 2′-deoxyribonucleic acid (DNA) repair in vivo are many and varied.[1] For example, it is well-known that cytosine (C) bases in DNA undergo spontaneous deamination in vivo to produce uracil (U) bases, the latter being foreign to normal DNA structure.[2] While the spontaneous conversion of C to U occurs infrequently ($k = 2 \times 10^{-10}$ s^{-1} for single-stranded DNA, $k = 1 \times 10^{-12}$ s^{-1} for double-stranded DNA),[1] this mutation threatens DNA sequence integrity and thus must be corrected efficiently. The initial repair step involves the removal of the uracil base via *N*-glycoside bond cleavage catalyzed by uracil-DNA glycosylase,[3-5] producing an apyrimidinic (AP) site in the DNA molecule. Subsequent processing by DNA polymerase and ligase excises the deoxy sugar and inserts the correct C residue.

The transient AP site is composed of 2-deoxy-α-D- and -β-D-*erythro*-pentofuranosyl rings (**1a** and **1b**, respectively) (Scheme I) linked to the DNA strand via two phosphodiester bonds. Using stable isotopically enriched DNA oligomers, Gerlt and co-workers[6,7] found that the anomeric distribution of **1** at an AP site generated in a single-stranded DNA oligomer was similar to that observed for 5-*O*-methyl-2-deoxy-D-*erythro*-pentose (**2**) (Scheme I) in aqueous solution. Recently Raap and co-workers[8] proposed that methyl 2-deoxy-α-D-*erythro*-pentofuranoside (**3a**) and methyl 2-deoxy-β-D-*erythro*-pentofuranoside (**3b**) are good conformational models of **1** in abasic DNA. A least-squares analysis[9a] of $^3J_{HH}$

Scheme I

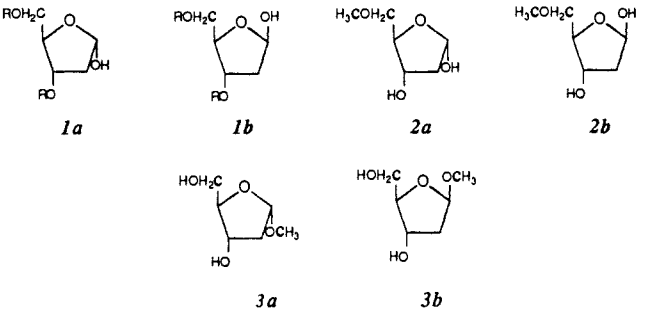

Table I. ^{1}H–^{1}H Spin-Coupling Constants[a] in 2-Deoxy-5-*O*-methyl-D-*erythro*-pentofuranoses in ^2H_2O at 25 °C

coupled nuclei	α-furanose **2a**	β-furanose **2b**
1,2	5.5 (5.4)[b]	5.1 (2.7)
1,2′	2.4 (1.3)	4.0 (5.5)
2,2′	−14.2	−14.0
2,3	7.1 (7.5)	5.7 (6.7)
2′,3	3.7 (2.5)	6.5 (5.9)
3,4	4.5 (3.6)	4.4 (4.2)
4,5	3.2	4.1
4,5′	6.0	7.2
5,5′	−11.0	−10.9

[a] Coupling constants are expressed in hertz and are accurate to ±0.1 Hz. [b] Values in parentheses are corresponding couplings reported previously for **3a** and **3b**[8] at 19 °C.

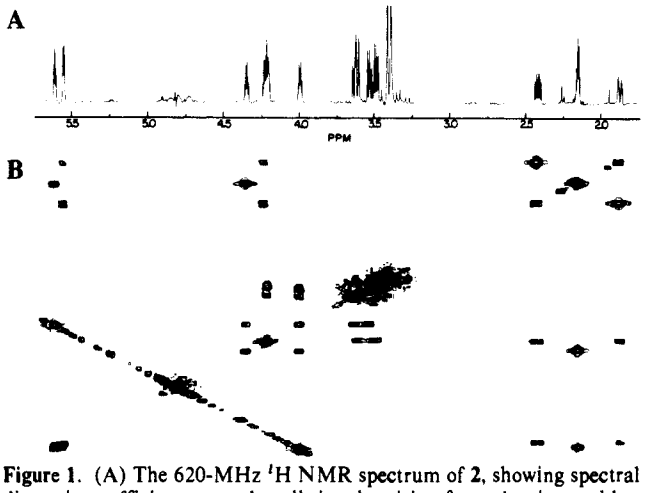

Figure 1. (A) The 620-MHz ^{1}H NMR spectrum of **2**, showing spectral dispersion sufficient to resolve all signals arising from the ring and hydroxymethyl protons of both anomers. Chemical shifts in parts per million relative to the internal HOD signal (4.80 ppm) are as follows: for **2a**, 5.50 (H1), 2.37 (H2), 1.83 (H2′), 4.17 (H3), 4.15 (H4), 3.56 (H5), 3.44 (H5′), 3.37 (CH_3); for **2b**, 5.55 (H1), 2.12 (H2), 2.09 (H2′), 4.29 (H3), 3.94 (H4), 3.58 (H5), 3.49 (H5′), 3.34 (CH_3). (B) The ^{1}H–^{1}H COSY spectrum of **2** obtained at 620 MHz used to assign specific proton multiplets to each anomer via the off-diagonal elements.

(1) For a recent review, see: Sancar, A.; Sancar, G. B. *Annu. Rev. Biochem.* **1988**, *57*, 29.
(2) The presence of uracil in DNA may also arise from misincorporation by DNA polymerase, or deamination of cytosine catalyzed by bisulfite ion or nitrous acid.[1]
(3) Lindahl, T. *Annu. Rev. Biochem.* **1982**, *51*, 61.
(4) Lindahl, T. *Prog. Nucleic Acid Res. Mol. Biol.* **1979**, *22*, 135.
(5) Friedberg, E. C. *DNA Repair*; Freeman Publishers: New York, 1985.
(6) Manoharan, M.; Ransom, S. C.; Mazumder, A.; Gerlt, J. A. *J. Am. Chem. Soc.* **1988**, *110*, 1620.
(7) Wilde, J. A.; Bolton, P. H.; Mazumder, A.; Manoharan, M.; Gerlt, J. A. *J. Am. Chem. Soc.* **1989**, *111*, 1894.
(8) Raap, J.; van Boom, J. H.; van Lieshout, H. C.; Haasnoot, C. A. G. *J. Am. Chem. Soc.* **1988**, *110*, 2736.
(9) (a) Haasnoot, C. A. G.; de Leeuw, F. A. A. M.; de Leeuw, H. P. M.; Altona, C. *Org. Magn. Reson.* **1981**, *15*, 43. (b) $^3J_{HH}$ in **3b** were found[8] to be independent of temperature over the range −2 to 73 °C.

0002-7863/90/1512-5886$02.50/0